DEVELOPMENT OF A CONTROL ALGORITHM FOR A MOLTEN-SALT SOLAR CENTRAL RECEIVER IN A CYLINDRICAL CONFIGURATION*

Gregory J. Kolb
Sandia National Laboratories
Albuquerque, New Mexico

ABSTRACT

A control algorithm is proposed for a molten-salt solar central receiver in a cylindrical configuration. The algorithm simultaneously regulates the receiver outlet temperature and limits thermal-fatigue damage of the receiver tubes to acceptable levels. The algorithm is similar to one that was successfully tested for a receiver in a cavity configuration at the Central Receiver Test Facility in 1988. Due to the differences in the way solar flux is introduced on the receivers during cloud-induced transients, the cylindrical receiver will be somewhat more difficult to control than the cavity receiver. However, simulations of a proposed cylindrical receiver at the Solar Two power plant have indicated that automatic control during severe cloud transients is feasible. This paper also provides important insights regarding receiver design and lifetime as well as a strategy for reducing the power consumed by the molten-salt pumps.

INTRODUCTION

Numerous studies and experiments by major U. S. utilities and the Department of Energy have defined the design of the next-generation solar central receiver power plant [1]. This power plant is characterized by a tower-mounted cylindrical-type receiver that is cooled by molten salt. The receiver is heated by reflected energy from a field of sun-tracking mirrors, called heliostats. Figure 1 shows a flow schematic of this system. Molten salt flows within the receiver tubes to be heated from 550 °F to 1050 °F (288 to 565 °C). The hot salt is sent to thermal storage where it is extracted for generation of steam in the steam generator. The steam powers the turbine to produce electricty. The cooled salt is returned through the thermal storage to the receiver. Molten salt was chosen as the preferred heat transfer fluid because it provides an efficient and low-cost thermal storage medium. Cost-effective storage allows the power plant to achieve high annual capacity factors (>60%) and to dispatch electricity to the grid when needed, even during cloudy weather or at night.

The subject of this paper is the control algorithm for the molten-salt receiver. Given variations in solar heat input to the receiver, the goals of the algorithm are to 1) maintain the salt at 1050 °F (565 °C) at the exit of the receiver, and 2) to limit thermal fatigue damage to the receiver tubes to ensure a 20-to-30 year lifetime. The algorithm accomplishes this by regulating the salt flow to match the solar heat impinging on the receiver. A control algorithm was developed and successfully demonstrated during the test of a molten salt receiver at the Central Receiver Test Facility (CRTF) in 1988 [2,3]. Outlet temperature was automatically controlled during clear and partly-cloudy weather conditions. In addition, thermal fatigue damage was limited by maintaining acceptable tube temperatures during the transients. In parallel with controls development, Sandia Laboratories and ESSCOR Corporation developed a simulation model of the receiver system and the control algorithm [6].

In 1991, a team of U. S. utilities led by Southern California Edison Company, expressed interest in installing molten salt equipment at the Solar One power plant. If this occurs, the new name of the plant will be Solar Two [4] and it could be on-line by 1994. The receiver at Solar Two will have a cylindrical geometry, which is significantly different than the cavity geometry tested at the CRTF in 1988. Because of the difference in shape, cloud transients will affect the receivers differently, and modifications to the control algorithm will be necessary.

In this paper, possible modifications to the original algorithm are investigated. This was done by converting the simulation model to mimic the Solar Two receiver system and studying the dynamic response of the receiver to a variety of cloud transients. In addition to identifying possible changes to the

*This work is supported by the Department of Energy under contract DE-AC04-76DP00789.

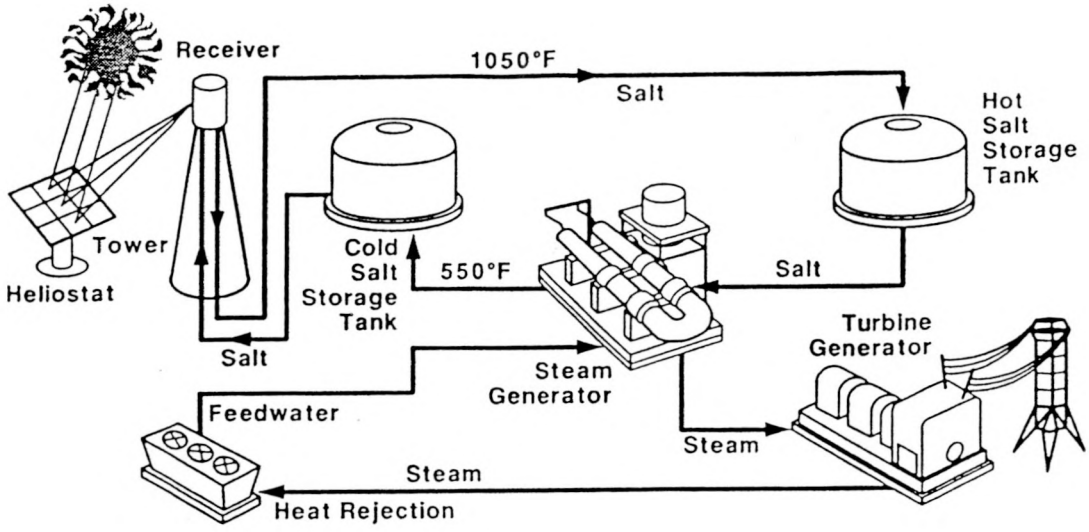

Figure 1 Schematic of a Molten-Salt Central Receiver Power Plant

algorithm, this paper also provides important insights regarding receiver design and lifetime as well as a strategy for reducing the power consumed by the molten-salt pumps.

DESCRIPTION OF THE SOLAR TWO RECEIVER SYSTEM

The receiver system analyzed here was proposed by Solar Power Engineering Company (SPECO) as part of the U. S. utility studies [5][1]. Like the water-steam receiver at Solar One, the Solar Two salt receiver is designed to absorb approximately 1.36 E08 Btu/hr (40 MW_t). However, because the salt receiver has a higher flux limit, it can absorb the same amount of energy with approximately one-half the surface area. Consequently, the receiver is one-half the height of Solar One's and measures 23 feet (7 m) in diameter by 24 feet (7.3 m) tall (see Figure 2a). Cold salt is pumped up the tower to the surge tank. The salt then enters the receiver from the north and hot salt exits from the south via two flow-control zones. There are 16 receiver panels per flow-control zone. After traversing four panels, the salt is routed to the opposite side of the receiver through a crossover pipe; there are therefore three crossover pipes per control zone (see Figure 2b). As explained later, these three pipes were included to increase daily performance. Each panel consists of 35 parallel tubes measuring 0.75 inch (19 mm) OD, 0.62 inch (15.7 mm) ID, and is made of 316 stainless steel. Total flow at the design point is 720,000 lb/hr (92 kg/sec).

---

[1]Modifications to the base-line design may be made before the receiver is installed at Solar Two in order to optimize performance. Control of modified designs should be reexamined, but it is likely that insights developed in this paper will be applicable to these future designs.

DESCRIPTION OF SIMULATION MODEL

The computer simulation of the Solar Two receiver system was developed based on a set of 127 ordinary differential equations (ODEs) that describe the time-varying behavior of the plant components, i.e., receiver, pumps, valves, tanks, controls. The model provides for the computation of temperatures, pressures, and flows when there are disturbances such as cloud passages over the heliostat field or component failures. The space dependence has been handled by sectionizing the system into several lumps (or nodes). Algebraic equations in the model may be eliminated by substitution, yielding the following simplified vector description:

$$\frac{d\bar{x}}{dt} = A\,\bar{x} + \bar{f}\,(\bar{x}, t) + B\,\bar{u}(t);\ X(0) = X_o \quad (1)$$

where

$\bar{x}$ = the state vector
A = a matrix of constant coefficients of the linear terms
$\bar{f}(\bar{x},t)$ = the vector of nonlinear and variable coefficient terms
$\underline{B}$ = a matrix of constant coefficients
u(t) = forcing function vector
X_o = vector of initial conditions

The basis for the Solar Two model was a similar equation set [6] developed for the molten salt cavity receiver tested at the CRTF in 1988. The model for the cavity receiver was validated with experimental data and was an excellent predictor of the actual performance of the cavity receiver [6]. Modifications to the simulation models included changes to the receiver subroutine to mimic a cylindrical geometry, alterations to the algorithm recommended in Reference

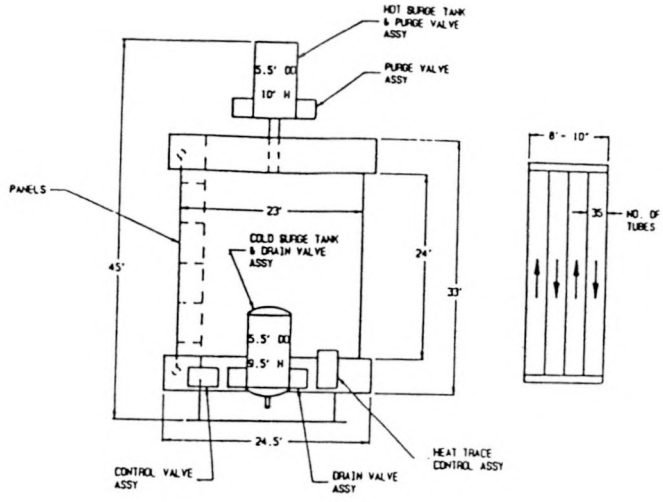

Figure 2a

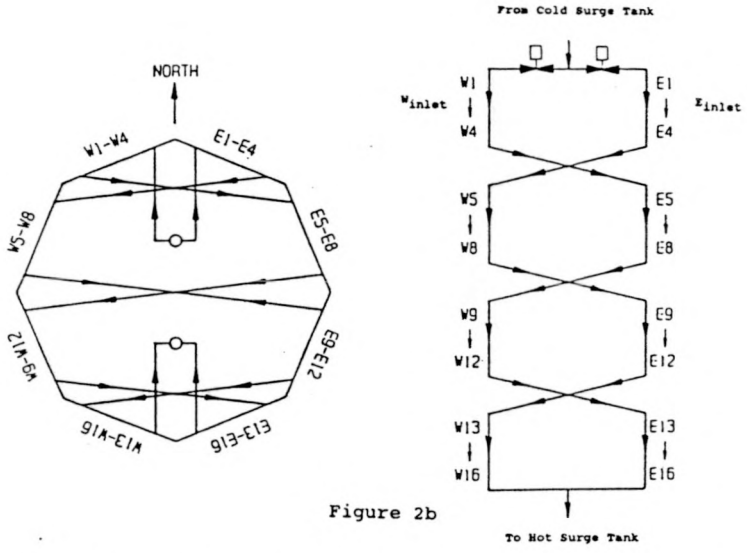

Figure 2b

Figure 2 Receiver Dimensions and Flow Circuitry Proposed by SPECO for the Solar Two Power Plant

2 to reduce tube strain, and recalculation of many plant-specific parameters (e.g. controller gain settings, tube properties).

New models were created to simulate cloud-induced transients and to obtain estimates of the dynamic strain experienced by the receiver tubes. These models are described in the following paragraphs.

Time-varying solar input to the receiver caused by cloud transients was simulated with a DELSOL3 [7] optics model of the combined heliostat and receiver systems at Solar Two. This model provides time-varying solar input to each of receiver panels as a function of time of day, day of year, and direction of cloud.

In addition to maintaining receiver outlet temperature at 1050 °F (565 °C), the control algorithm must protect the receiver tubes from thermal-fatigue damage. This can be accomplished by maintaining the axial strain of the tube within acceptable limits. Axial strain is a function of the temperature gradient between the front and back of the tube and can be written as [8]:

$$\varepsilon = a\,\{(T_c+T_{ci})/2-[T_s+.318((T_c+T_{ci})/2-T_s)] + (T_c-T_{ci})/2(1-\nu)\} \qquad (2)$$

where

ε = total strain
a = coefficient of thermal expansion
T_c = tube crown temperature
T_{ci} = inside tube crown temperature
T_s = bulk salt temperature = back tube temperature
ν = Poisson's ratio

T_c and T_{ci} are determined from a standard equation describing heat transfer through the wall of the tube and are evaluated at the point on the tube exposed to the maximum solar flux.

The strain is considered to be acceptable if the strains experienced by the receiver tubes, during a transient, are less than the allowable strain established for a 30-year lifetime. For tubes made of 316 SS, the allowable strain as a function of temperature is plotted in Figure 3 [14]. For reference, the strain experienced by the tubes at the design-point time, noon on equinox, for the SPECO receiver are presented in Table 1. By comparing Table 1 and Figure 3 it can be seen that the design point strain is significantly less than the allowable strain. Since the SPECO receiver is oversized relative to the optimum size identified in the Utility Study [1], the average and peak solar flux on the receiver is less which causes a corresponding drop in strain. However, it is possible to approach the allowable strain by changing the aiming strategy for the heliostats to increase the peak-panel fluxes and temperatures on the receiver. Analysis with DELSOL indicates that reaiming can increase the peak flux listed in Table 1 by as much as 70%.

The simulation model was programmed on a personal computer (PC) with the System Simulation Language (SYSL) [9]. The model runs real time on a 286-based PC with a 12 MHz clock. When the simulator is running, a graphics interface appears on the monitor which allows the user to modify selected variables at any time.

Table 1

Tube Strain at Design Point for the Panels on the Solar Two Receiver Proposed by SPECO

Panel Number	Peak Absorbed (MW/m^2)	Peak Tube Temp. (°F)	Strain
2 (North)	430	858	.0019
4	420	920	.0017
6	400	982	.0015
8	370	1034	.0013
10	320	1069	.0011
12	250	1083	.0008
14	190	1094	.0006
16 (South)	150	1104	.0004

DESCRIPTION OF CONTROL ALGORITHM

The proposed control algorithm for the Solar Two receiver is displayed in Figure 4. This algorithm is similar to the final one developed during the Phase II testing of the cavity receiver at the CRTF [3]. The goal of the algorithm is to simultaneously maintain tube strain within acceptable limits and regulate outlet salt temperature to 1050 °F (565 °C). Three independent control signals are used to regulate the salt flow in each of two flow-control zones. They are

1. a feedforward signal from the solar power on the receiver,
2. a feedback signal from the average-back-tube temperature,
3. a feedback signal from salt-outlet temperature.

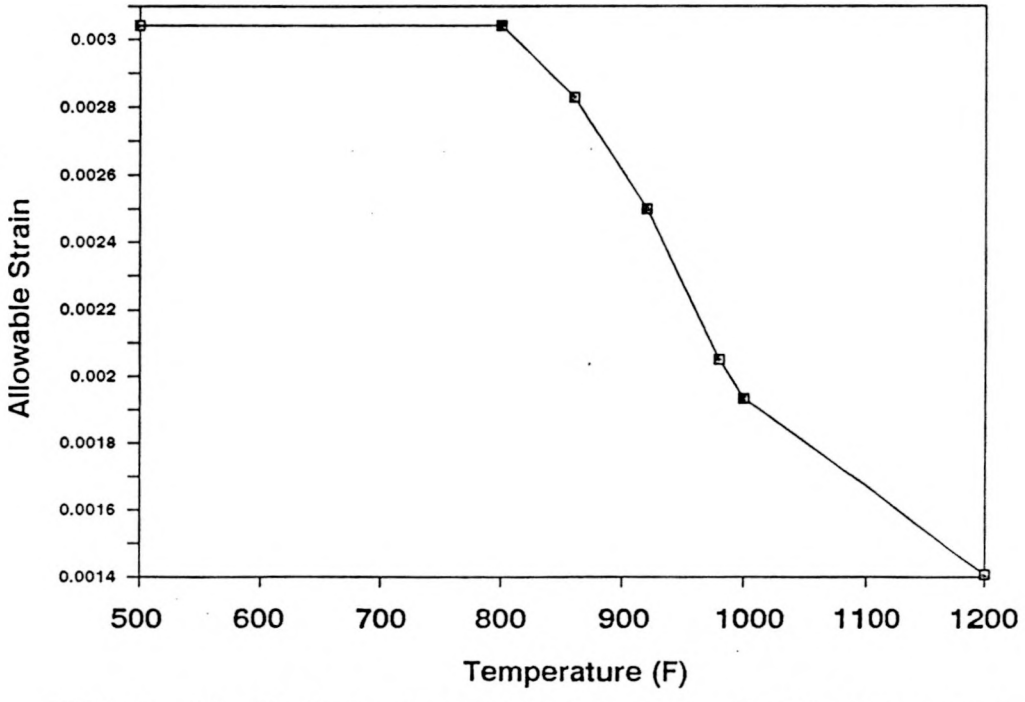

Figure 3 Allowable Strain as a Function of Temperature for 316 Stainless Steel to Achieve a 30 Year Lifetime (30,000 Design-Point Thermal Cycles)

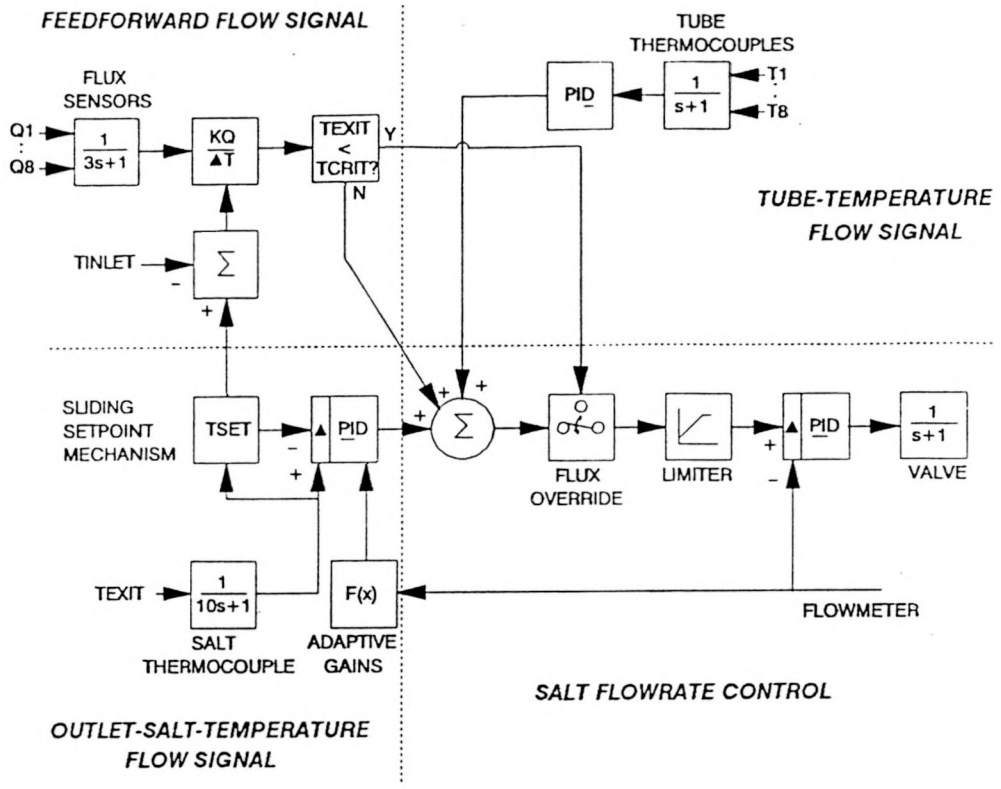

Figure 4 Proposed Control Algorithm for the Solar Two Receiver

The three signals are summed to provide a total flow setpoint on the porportional-plus-integral controller which regulates the flow control valve to achieve that setpoint. The signals are listed above in order of their flow-control authority. The feedforward signal is the most authoritative since it changes flowrate simultaneously with solar flux changes. The temperature signal from the back of the tubes is the next most authoritative, since there is knowledge of temperature changes along the entire flow path. The influence of the outlet-salt temperature signal is felt last because its knowledge is limited to only exit conditions, which occur after an extended residence time of the fluid.[2]

Adaptive gains are utilized to modify the proportional and integral gain as a function of flow rate in the salt-outlet temperature controller. The exit temperature setpoint is also ramped between a low value (assumed to be 950 °F (510 °C) in the cases analyzed here) and 1050 °F (565 °C). This "sliding setpoint mechanism" prevents high temperature trips of the receiver during cloud transients.

For the case of an extended cloud cover, the outlet temperature will approach the inlet salt temperature of 550 °F (288 °C) within approximately 6 minutes. When the cloud clears the heliostat field, it is important to quickly ramp the flow to near its maximum value to maintain tube strains within acceptable limits. To accomplish this, the outlet-salt temperature and tube temperature flow signals are bypassed and reset to zero, and only the feedforward signal is used. This operating mode is called "flux override." Bypassing the other signals prevents them from holding back the flow due to controller windup, i.e., during an extended cloud cover the integrator in the outlet-temperature controller will produce a large negative flow signal, which could hold back flow if not bypassed and reset to zero.

[2]Simulations indicate that at full flow, about 90 seconds are required for a step temperature change in the inlet to be completely felt at the outlet. The values are about the same for the cylindrical receiver at Solar Two and the cavity receiver tested at the CRTF.

SIMULATION OF CLOUD-INDUCED TRANSIENTS

Cloud passages from several different directions were examined with the simulation model. The most difficult to control is a cloud that clears the heliostat field from north to south.[3] In this situation the flux appears on the receiver in the direction of the salt flowing through it, and the delay between initial flux and rise in outlet temperature is the longest. The importance of the flux-feedforward signal is paramount, given this cloud passage, to prevent a high-temperature trip of the receiver at 1090 °F (588 °C) and to protect the receiver from thermal fatigue damage.

Presented in Figure 5 is the response of outlet salt temperature and flow rate for one of two control

[3]Simulation of clouds from east to west and from south to north verified this to be true.

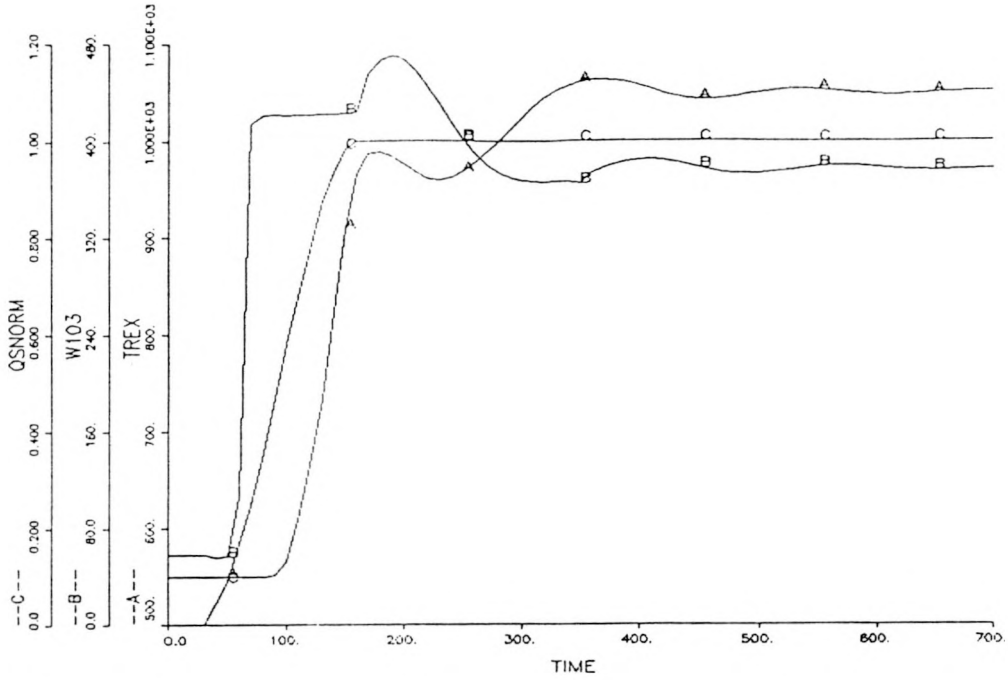

Figure 5 Response of the SPECO Receiver to a North-to-South Cloud Moving at 11 mph -- Normalized Solar Power on Receiver (QSNORM), Salt Flowrate (W103, Klb/hr), Outlet Salt Temperature (TREX, °F)

zones given a cloud traveling at 11 mph (the speed used to tune the algorithm for the cavity receiver tested at the CRTF). The cloud, represented on the figure as normalized solar power, begins clearing the field at t = 30 seconds and takes 2 minutes to completely clear. Flow begins to increase at t = 50 seconds and the "flux override" feature of the algorithm quickly ramps flow to a level determined by the feedforward signal and the lower limit (950 °F (510 °C)) of the sliding setpoint mechanism. Flow is maintained at that level until the outlet temperature exceeds 950 °F at t = 170 seconds, at which point the sliding setpoint begins to travel upward to the desired outlet temperature of 1050 °F (565 °C). The feedback controller is activated to maintain this desired temperature.

The axial strains experienced by the receiver tubes are displayed in Figure 6. The values are normalized relative to the allowable strain curve (Figure 3). Since all strains are less than unity, overstrain of the receiver tubes did not occur. To accomplish this, flow was ramped to full when the flux on any one of the panels exceeded 50% of the previous steady-state value. Since the cloud cleared from the north, this was detected by the flux sensor on the north receiver panel. Sensitivity studies were used to select the point at which flow should be ramped. For example, waiting until flux exceeds 60% results in a 35% overstrain.

The need to ramp the flow based on the flux input from a single panel is a difference between the control of a cavity and cylindrical receiver. The control algorithm for the cavity receiver ramped the flow based on an average flux signal from all the panels. This approach was tried for the cylindrical receiver and resulted in a trip on high outlet salt temperature and/or a severe overstrain of the receiver tubes. The two receivers respond differently because of the difference in the way flux is brought onto the receiver. For the cylindrical receiver, several of the panels can remain dark for an extended period because each panel only views a selected portion of the heliostat field. For the cavity receiver, each panel views a much larger section of the heliostat field, and all panels soon see some light from the field. Though the total power on the receiver as a function of time is the same for both receivers, the power on the cavity receiver is more uniformly distributed during the cloud passage. It is easier to control a receiver when solar energy is brought onto it in a uniform fashion. In addition, full solar power will be brought onto certain receiver panels more quickly for a cylindrical geometry than for a cavity geometry. For example, during a north-to-south cloud passage, peak solar flux will be seen on the north panel of a cylindrical receiver when only the northern portion of the heliostat field is uncovered. With a cavity geometry, peak solar flux is not seen on the receiver until the entire field is uncovered.

INSIGHTS REGARDING DESIGN AND LIFETIME OF THE RECEIVER SYSTEM

Tube Lifetime

A receiver is usually designed for a 30-year life. During that time it is typically assumed the receiver will experience the equivalent of 30,000 cycles at the design point condition [12]. To last 30 years, tube strain must be kept within acceptable limits during cloud transients, otherwise thermal cycling damage will significantly reduce the life of

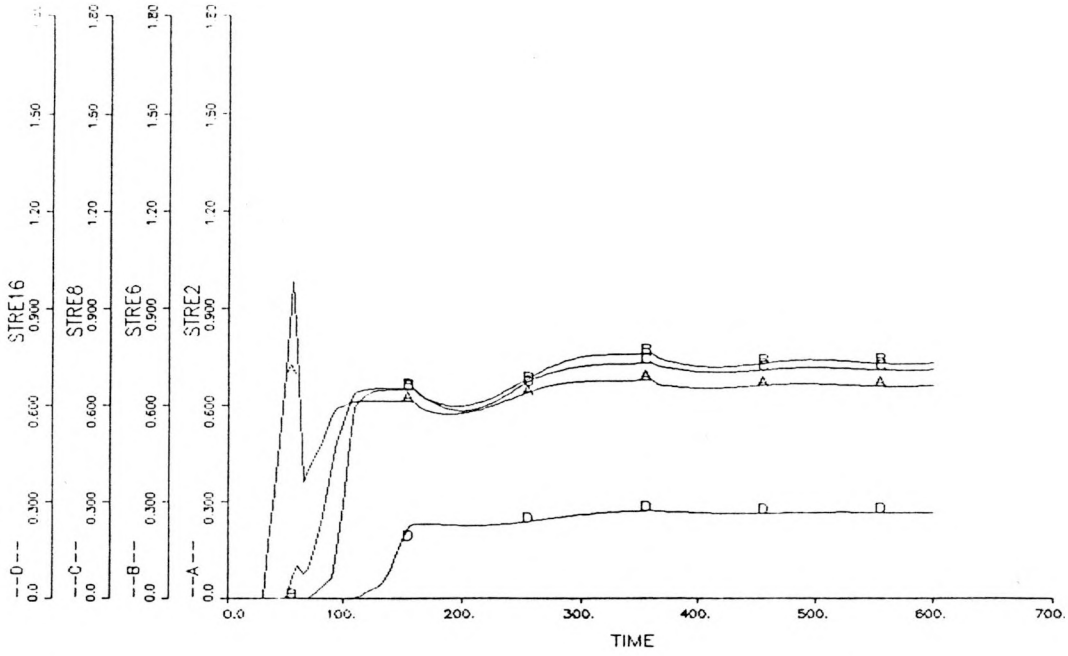

Figure 6 Normalized Strains for Tubes Within Solar Two Receiver Panels 2, 6, 12, and 16 During North-to-South Cloud Transient

the receiver [10]. The control algorithm described in the previous section appears to be capable of achieving this.

Panel Header Design

The receiver should be designed to accommodate significant temperature ramp rates. This will occur during rapid heatup and cooldown of the receiver during cloud transients. Plotted in Figure 7 are the tube-temperature derivatives during the north-to-south cloud transient described in the previous section. It can be seen that peak ramp rates range from 8 to 10 °F (4.4 to 5.5 °C) per second. Such ramp rates have been overlooked by receiver designers in the past; a problem area is the welded junction between the thin receiver tubes and the thicker panel header. [11]. However, receiver designers [13] state that it is possible to design the junction to withstand a particular ramp rate. Based on the analysis conducted here, it is recommended that the interface be designed to withstand short-term ramp rates of at least 10 °F (5.5 °C) per second. Another option is to reduce ramp rates by removing a fraction of the heliostats from the receiver during a cloud transient and bringing them back on the receiver when the cloud clears. For example, sensitivity studies indicated that removal of 50% of the heliostats lowered the peak ramp rate by approximately 50%. However, removal of heliostats during cloudy weather is not the preferred solution because it complicates the control algorithm, causes energy to be lost, and creates a corresponding drop in system efficiency.

Panel Crossover Design

As discussed previously, the base-line receiver design developed by SPECO employed three crossover pipes. This was done to equalize the total solar power absorbed by the two control zones at different times of the day. This can be best explained by viewing Table 2 and Figure 2b. Table 2 compares the power absorbed by the two control zones (designated W_{inlet} and E_{inlet}) given that 0, 1, or 3 crossovers per control zone are used. It can be seen that at noon on the summer solstice, 7 E07 Btu/hr (20.5 MW_t) is absorbed by each control zone. The power for each zone is the same at noon because the flux on the receiver is symmetric about a north-to-south centerline. At 6 p.m. on the same day, however, the flux pattern on the receiver is skewed such that more flux is on the eastern half of the receiver. If no crossovers are used, there is a factor of 2 difference between the power absorbed by each of the control zones. If three crossovers are used, the power absorbed by each zone is nearly the same. Equalizing the flow increases the length of time the receiver may

Table 2
Comparison of Total Solar Power (MW_t)
Absorbed in Each Solar Two Control Zone
as Predicted by the DELSOL3 [7] Computer Code

Solar Day	Solar Time	0 Crossovers Win	0 Crossovers Ein	1 Crossovers Win	1 Crossovers Ein	3 Crossovers Win	3 Crossovers Ein
Summer Solstice	Noon	20.5	20.5	20.5	20.5	20.5	20.5
	4 p.m.	11.6	18.6	14.6	15.6	15.0	15.2
	6 p.m.	2.8	5.5	3.6	4.8	4.1	4.3
Equinox	Noon	20.2	20.2	20.2	20.2	20.2	20.2
	5 p.m.	3.3	6.0	4.5	4.8	4.8	4.5
Winter Solstice	Noon	18.7	18.7	18.7	18.7	18.7	18.7
	3 p.m.	8.2	11.3	10.2	9.2	9.8	9.7

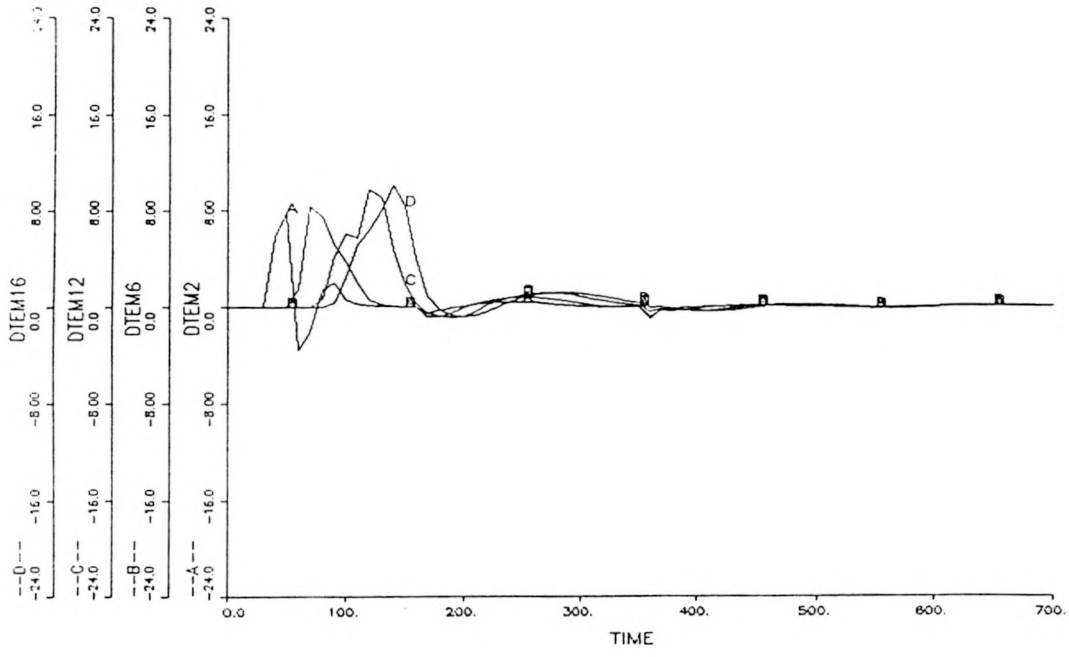

Figure 7 Ramp Rates (°F/sec) for Tubes Within Solar Two Receiver Panels 2, 6, 12, 16 During North-to-South Cloud Transient

operate during the day. For example, with no crossovers, the receiver would probably be shut down at 6 p.m. on the summer solstice because the salt flow within W_{inlet} was below the minimum allowable (flow at 6 p.m. is ~2.8/20.5 = 13.7%, and minimum allowable, based on thermohydraulic concerns, is typically 15%). Adding crossovers increases flow above the minimum allowable. Returning to Table 2 it can be seen that, on an annual basis, one crossover is nearly as effective as three. Because of this, it is recommended that one crossover per control zone be used rather than three. Referring to Figure 2b, the E_{inlet} crossover would connect panels E8 and W9, and W_{inlet} crossover would connect panels W8 and E9. Besides reducing design complexity and cost, a single crossover improves the controllability of the receiver during cloud transients because the salt transit time is reduced. The simulations presented in the previous section were based on a single crossover.

Reduction of Electrical Parasitics

The electrical energy consumed by the cold-salt pumps is one of the largest parasitic loads at a central receiver power plant. It is important to reduce the energy consumed by these pumps, to the extent possible, to improve the overall efficiency of the power plant. The electric power consumed by the cold pumps is a function of the tower height, the pressure drop across the receiver, and the the operating pressure of the cold-surge tank. At Solar Two, the tower height is fixed at 285 feet (87 m). It is anticipated that optimization studies will be conducted in the future to select the ideal receiver-pressure drop and cold-surge operating pressure. The insights presented below should be useful to these studies.

To assure a safety margin in controlling the receiver, it is desirable to have some overcooling capability. In other words, the cold salt pumps should be able to maintain the salt exit temperature below 1050 °F (565 °C) when design point power is incident on the receiver. In this paper, the cold pumps were sized to maintain the outlet temperature at approximately 950 °F (510 °C) with the pumps operating at full flow. However, the overcooling capability is achieved at the cost of installing a larger and more expensive cold pump, as well as higher pumping parasitics.

The pressure drop for the SPECO receiver analyzed in this paper is 430 psi (3 MPa) when operating at the design point conditions within a flow control zone: 7E07 Btu/hr (20 MW_t), 1050 °F (565 °C) outlet temperature, 100 lb/sec (46 kg/sec). To achieve an outlet temperature of 950 °F (510 °C) with 20 MW_t on a control zone, the required flow rate is 130 lb/sec (60 kg/sec). Since pressure drop increases as the square of the salt velocity, the pressure drop will increase to approximately 710 psi (4.9 MPa) when flowing at 130 lb/sec. Assuming a 100 psi (0.69 MPa) drop across the flow control valve and other losses in the piping, the air space within the cold surge tank should be pressurized to about 825 psi (5.7 MPa). With the surge tank at this pressure, the parasitic power required by the cold salt pumps is 2.3 E06 Btu/hr (670 kW), or 6.7% of the nameplate rating for the Solar Two turbine generator. If no overcooling capability existed, the surge tank would operate at a lower pressure (~540 psi (3.7 MPa)) and the parasitic power would be reduced to about 1.2 Btu/hr (350 kW).

It is undesirable to maintain the surge tank pressure at a high pressure (825 psi (5.7 MPa) for the case analyzed here) throughout the entire operating day. Early and late in the day when insolation and the corresponding salt-flow rate are significantly lower than the design-point value, the pressure drop

across the receiver will also be considerably less. During these times the pressure in the cold surge tank could be lowered and the speed of the cold salt pumps decreased to reduce parasitics. The tank pressure would be selected to retain some overcooling capability. This feature could be incorporated into the control algorithm through a table look-up function, which selects the correct pressure as a function of time of day and day of year.

CONCLUSIONS

Based on an analysis of a proposed receiver for the Solar Two Power Plant, it appears that automatic control of a cylindrical-type receiver during cloud-induced transients is feasible. The control algorithm simultaneously regulates outlet temperature and maintains tube strain within acceptable limits. To accomplish this, a few modifications to the algorithm developed previously for the cavity receiver were necessary.

Insights were also developed regarding receiver design: 1) a single crossover per control zone appears adequate, 2) interfaces between receiver tubes and panel headers should be designed to accommodate tube-metal ramp rates of at least 10 °F (5.5 °C) per second, and 3) variable pressure control in the cold-surge tank could be used to reduce cold pump parasitics.

We will continue to use the simulation model described in this paper to test new ideas regarding the optimization of the design for Solar Two. For example, we will evaluate receiver designs with different tube geometries and panel configurations. We also plan to investigate the effect that higher peak fluxes and cloud speeds have on controllability of the receiver as well as innovative control strategies and receiver designs that eliminate crossover pipes.

REFERENCES

1. Pacific Gas & Electric Company, Solar Central Receiver Technology Advancement for Electric Utility Applications, Phase 1 Topical Report, Report No. 007.2-88.2, San Francisco, CA, September 1988.

2. Grossman, J. W., E. S. Riley, J. M. Chavez, R. F. Boehm, "Phase II Testing of a Molten Salt Central Receiver," (conference paper), Solar Thermal Technology: Research Development and Applications, B. P. Gupta (editor), Hemisphere Publishing Company, 1990.

3. Riley, E. S., Phase II Testing of a Molten Salt Central Receiver, (full report), Automated Control Systems, Inc., Albuquerque, NM, draft report, 1988.

4. Alpert, D. J., G. J. Kolb, J. M. Chavez, "Today's Central Receiver Power Plant," SAND91-1890C, Proceedings of the 1991 International Solar Energy Society Conference, Denver, CO, 1991.

5. Tracey, T. R., O. Scott, and M. Brzeczek, "Design of a Molten Nitrate Salt Receiver for Solar One," Solar Power Engineering Company, Proceedings of Twelfth Annual ASME International Solar Energy Conference, Miami, Florida, 1990.

6. Kolb, G. J., D. T. Neary, M. R. Ringham, T. L. Greenlee, Dynamic Simulation of a Molten-Salt Solar Receiver, SAND88-2895, Sandia National Laboratories, Albuquerque, NM, 1989.

7. Kistler, B. L., A User's Manual for DELSOL3: A Computer Code for Calculating the Optical Performance and Optimal System Design for Solar Thermal Central Receiver Plants, SAND86-8018, Sandia National Laboratories, Livermore, CA, 1986.

8. Babcock & Wilcox Company, Molten Salt Receiver Subsystem Research Experiment Phase 1 - Final Report, Volume 1 - Technical, SAND82-8178, Sandia National Laboratories, Albuquerque, NM, 1984.

9. E² Consulting, System Simulation Language User's Guide, SYSL/M Version 2.0, Poway, CA, 1987.

10. Grossman, J. W., W. B. Jones, P. S. Veers, "Evaluation of Thermal Cycling Creep-Fatigue Damage for a Molten Salt Receiver," Sandia National Laboratories, Proceedings of Twelfth Annual ASME International Solar Energy Conference, Miami, Florida, 1990.

11. Chavez, J. M., and D. C. Smith (editors), Molten Salt Subsystem/Component Experiment: Receiver Subsystem Test Final Report, Volume II - Report, SAND87-2290, Sandia National Laboratories, Albuquerque, NM, 1987, draft report.

12. Kistler, B. L., Fatigue Analysis of a Solar Central Receiver Design Using Measured Weather Data, SAND86-8017, Sandia National Laboratories, Livermore, CA, 1987.

13. Smith, D. C., Science Applications International Inc., Albuquerque, NM, personal communication, October, 1991.

14. Tyner., C. E., memo to distribution, "Summary of Workshop on Central Receiver Tube Life Considerations," Sandia National Laboratories, Albuquerque, NM, December, 17, 1986